Myosin VI is required for sorting of AP-1B–dependent cargo to the basolateral domain in polarized MDCK cells

Josephine Sui-Yan Au,[1] Claudia Puri,[2] Gudrun Ihrke,[2] John Kendrick-Jones,[1] and Folma Buss[2]

[1]Medical Research Council Laboratory of Molecular Biology, Cambridge CB2 2QH, England, UK
[2]Cambridge Institute for Medical Research, University of Cambridge, Cambridge CB2 0XY, England, UK

In polarized epithelial cells, newly synthesized membrane proteins are delivered on specific pathways to either the apical or basolateral domains, depending on the sorting motifs present in these proteins. Because myosin VI has been shown to facilitate secretory traffic in nonpolarized cells, we investigated its role in biosynthetic trafficking pathways in polarized MDCK cells. We observed that a specific splice isoform of myosin VI with no insert in the tail domain is required for the polarized transport of tyrosine motif containing basolateral membrane proteins. Sorting of other basolateral or apical cargo, however, does not involve myosin VI. Site-directed mutagenesis indicates that a functional complex consisting of myosin VI, optineurin, and probably the GTPase Rab8 plays a role in the basolateral delivery of membrane proteins, whose sorting is mediated by the clathrin adaptor protein complex (AP) AP-1B. Our results suggest that myosin VI is a crucial component in the AP-1B–dependent biosynthetic sorting pathway to the basolateral surface in polarized epithelial cells.

Introduction

In polarized epithelial cells, the plasma membrane is divided into functionally and morphologically distinct apical and basolateral domains that have different protein and lipid compositions and are separated by tight junctions. The polarized distribution of proteins is achieved by the sorting of newly synthesized proteins at the TGN and/or the recycling endosome into separate carriers destined for the apical or basolateral domain (Mostov et al., 2000). In addition, recycling proteins are sorted in the endosomal compartment after endocytosis from the plasma membrane. Sorting of basolateral transmembrane proteins is guided by peptide motifs present in their cytoplasmic tails, such as dileucine motifs or tyrosine-containing sequences, including YxxΦ and other less well-characterized signals (Muth and Caplan, 2003; Rodriguez-Boulan et al., 2005). Some, if not all, of these motifs bind to the clathrin adaptor protein complexes (AP)-1 and/or -4, which mediate incorporation of the cargo protein into basolateral carriers. Sorting to the apical domain is less well defined and may involve several pathways; depending on the specific membrane protein, it may require glycosylation of its extracellular domain, lipid raft association, or the presence of cytoplasmic peptide sequences (Muth and Caplan, 2003; Rodriguez-Boulan et al., 2005).

Polarized epithelial cells express a specific variant of AP-1, called AP-1B, which is important for basolateral targeting of several transmembrane proteins, including vesicular stomatitis virus glycoprotein G (VSV-G) and the low-density lipoprotein receptor (LDLR; Folsch et al., 1999; Ohno et al., 1999; Gan et al., 2002; Sugimoto et al., 2002). Both of these proteins contain tyrosine-dependent sorting motifs (Matter et al., 1992, 1994; Thomas et al., 1993). In contrast, sorting of the Fc γ receptor isoform BII (FcγRIIB), which contains a dileucine motif, appears to be AP-1B independent (Hunziker and Fumey, 1994; Matter et al., 1994; Roush et al., 1998; Folsch et al., 1999). Other components involved in basolateral transport are the actin-regulatory GTPase cdc42, the exocyst complex, and the GTPase Rab8. Functional defects caused by overexpression of cdc42 mutants highlight the importance of the actin cytoskeleton for transport of proteins from the TGN to the basolateral domain (Kroschewski et al., 1999; Musch et al., 2001). The exocyst is a protein complex of eight subunits that mediates the

Correspondence to F. Buss: fb1@mole.bio.cam.ac.uk

J. Au's present address is Cancer Research UK, Cambridge Research Institute, Li Ka-Shing Centre, Cambridge CB2 0RE, England, UK.

G. Ihrke's present address is Dept. of Pharmacology, Uniformed Services University of the Health Sciences, F. Edward Hébert School of Medicine, Bethesda, MD 20814.

Abbreviations used in this paper: AP, adaptor protein complex; CIMR, Cambridge Institute for Medical Research; FcγRIIB, Fc γ receptor isoform BII; LDLR, low-density lipoprotein receptor; LI, large insert; NI, no insert; SI, small insert; TfR, transferrin receptor; VSV-G, vesicular stomatitis virus glycoprotein.

The online version of this article contains supplemental material.

The Journal of Cell Biology, Vol. 177, No. 1, April 9, 2007 103–114
http://www.jcb.org/cgi/doi/10.1083/jcb.200608126

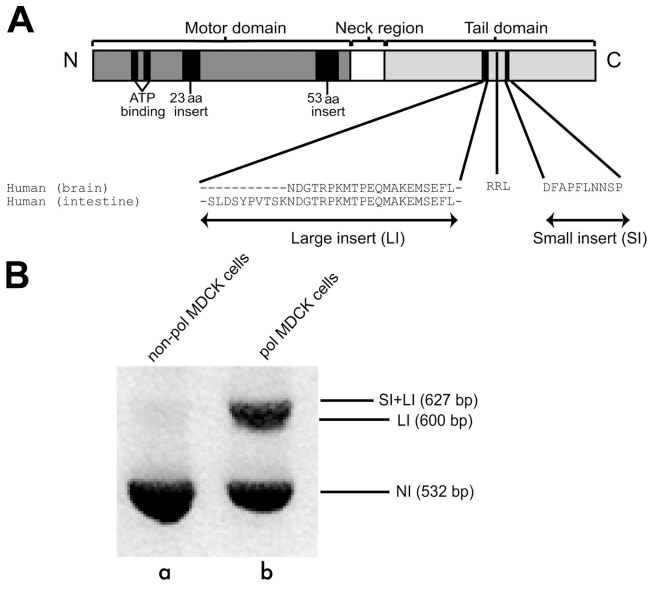

Figure 1. **Expression of myosin VI isoforms in MDCK cells.** (A) Schematic diagram of myosin VI domain organization. The motor domain contains two unique inserts; the 23-aa insert modulates its ATPase activity and the 53-aa insert is the "reverse gear" that controls its directionality along actin filaments. The tail domain is alternatively spliced with two insertions, a LI at the end of the helical domain and a SI within the globular domain. A long version (31 aa) of the LI isoform is expressed in MDCK cells, whereas the SI sequence is conserved between MDCK cells and human brain. (B) Expression of myosin VI isoforms in nonpolarized and polarized MDCK cells. Nonpolarized MDCK cells mainly express the myosin VI isoform with NI (a), whereas MDCK cells grown on filters for 4 d express three different isoforms with NI, the LI, and the SI+LI (b).

tethering of secretory vesicles to docking sites on the plasma membrane. In MDCK cells, this exocyst complex is required for delivery of membrane proteins to the basolateral domain, but not the apical domain (Grindstaff et al., 1998). In yeast, the function of the exocyst complex is regulated by the Rab GTPase Sec4 (Guo et al., 1999). The mammalian homologue of Sec4 is Rab8, which is a key regulator of exocytic membrane traffic from the Golgi complex to the plasma membrane (Huber et al., 1993; Moritz et al., 2001). In polarized MDCK cells, Rab8 specifically regulates AP-1B–dependent transport to the basolateral domain (Ang et al., 2003). In these cells, Rab8 and AP-1B can be found in recycling endosomes, which is an important sorting station for certain basolateral proteins that are en route to the plasma membrane (Ang et al., 2004). In nonpolarized cells, Rab8 has been shown to bind to optineurin, a conserved 67-kD protein containing multiple leucine zipper domains and a putative zinc finger, which also binds to myosin VI (Hattula and Peranen, 2000; Sahlender et al., 2005).

Myosin VI is a unique, actin-based motor protein that moves along actin filaments in the opposite direction of all the other classes of myosins characterized thus far (Wells et al., 1999). This multifunctional motor protein is involved in both endocytic and exocytic membrane-trafficking pathways (Buss et al., 1998, 2001; Aschenbrenner et al., 2003; Warner et al., 2003). Functional studies on nonpolarized cells derived from the myosin VI knock-out mouse (Snell's waltzer) have shown that myosin VI is required for efficient secretion of alkaline phosphatase and for the maintenance of Golgi morphology (Warner et al., 2003). In normal nonpolarized cells, myosin VI is linked to the Golgi complex and to the secretory pathway by optineurin because knockdown of optineurin by siRNA results in the loss of myosin VI from the Golgi complex and impaired delivery of VSV-G to the plasma membrane (Sahlender et al., 2005). Optineurin appears to be a linker protein between myosin VI and Rab8, as all three proteins colocalize in the perinuclear region at/around the Golgi complex and on vesicles underneath the plasma membrane. Overexpression of constitutively active Rab8Q67L recruits myosin VI onto Rab8-positive tubules and vesicles around the Golgi complex.

Four splice variants of myosin VI are expressed in mammalian cells in a tissue-specific manner; isoforms containing a large insert (LI) in the tail are found in polarized epithelial cells with well-developed apical microvilli, whereas isoforms with a small insert (SI) or no insert (NI) in the tail are expressed in polarized and nonpolarized cells (Buss et al., 2001). Because myosin VI is involved in the secretory pathway in nonpolarized cells and is linked via optineurin to Rab8, which regulates basolateral transport in polarized epithelial cells, we investigated the role of myosin VI in polarized biosynthetic membrane traffic in MDCK cells. We observed that the specific isoform of myosin VI with no inserts in the tail domain is required for transport of newly synthesized basolateral membrane proteins to the correct surface domain. Overexpression of the tail domain of this myosin VI isoform selectively inhibits delivery of tyrosine motif–containing cargo to the basolateral surface, but not that of basolateral membrane proteins with a dileucine motif or of membrane proteins with different apical sorting motifs. Thus, only the specific delivery of AP-1B–dependent basolateral cargo is inhibited. Site-directed mutagenesis indicates that a functional complex containing myosin VI, optineurin, and Rab8 mediates sorting along this transport pathway. Furthermore, we show that myosin VI and optineurin colocalize with AP-1, and also with Rab8 and the transferrin receptor (TfR) in clathrin-coated endosomal structures, which are therefore most likely to be recycling endosomes. Our results demonstrate that myosin VI is directly involved in the AP-1B–dependent sorting of proteins to the basolateral plasma membrane in polarized epithelial cells. This is the first motor protein to be identified in this pathway.

Results

Three different myosin VI isoforms are expressed in polarized MDCK cells

In mammalian cells, four splice variants of myosin VI are expressed, containing either a LI (21–31 aa), a SI (9 aa), both inserts (SI+LI), or NI in the C-terminal tail domain (Fig. 1 A). The tissue distribution of these isoforms indicates that the isoform containing the LI is predominantly expressed in tissues with polarized epithelial cells containing apical microvilli. To determine which of the myosin VI isoforms are expressed in nonpolarized and polarized MDCK cells, we performed RT-PCR on MDCK cells grown on normal tissue culture plasticware (nonpolarized cells) and on MDCK cells grown on porous filters (polarized cells), respectively. The RT-PCR results show

that nonpolarized MDCK cells contain the myosin VI isoform with NI, whereas the polarized cells express three different isoforms containing either NI, the LI, or the SI+LI (Fig. 1 B). Sequencing the RT-PCR products revealed that MDCK cells express a myosin VI with a longer 31-aa version of the LI compared with the LI expressed in human brain (21 aa) myosin VI. The sequences of the SI, however, were conserved between the myosin VI isoforms in MDCK cells and human brain.

The subcellular localization of myosin VI in MDCK cells

As a first step to elucidate the function of myosin VI in MDCK cells, we studied the subcellular localization of endogenous myosin VI by indirect immunofluorescence using a polyclonal antibody to the tail domain of myosin VI (Fig. 2 A). Endogenous myosin VI can be found throughout the cell at the apical and basolateral domains, but is slightly enriched in the apical terminal web region. To determine whether the three myosin VI isoforms expressed in polarized MDCK cells display a specific intracellular localization, we made stable MDCK cell lines expressing the corresponding human isoforms with an N-terminal GFP tag. For functional studies, we also raised a complete set of stable MDCK cell lines expressing the four different tail domain isoforms tagged with GFP, which can act as dominant-negative inhibitors of myosin VI function (Buss et al., 2001). At least four individual clones were raised for each isoform, and the highest expressing cells of each clone were enriched by FACS sorting. Immunoblotting results show that the amount of expressed GFP-tagged myosin VI (Fig. 2 B, top band) or tail (Fig. 2 B, bottom band) roughly equals the expression level of endogenous myosin VI.

Expression of the exogenous myosin VI variants (full-length or tail domains) did not appear to affect the ability of the cells to polarize when grown on a filter support. All clones showed very similar values for their transepithelial resistance compared with wild-type MDCK cells after 4 d of polarization. Moreover, in all clones, the zonular occludens-1 staining formed a continuous junctional pattern at the periphery of the cells, indicating that tight junction assembly was not compromised by the expression of any of the full-length myosin VI (NI, SI, LI, or SI+LI) or the four dominant-negative tail isoforms (unpublished data).

The full-length myosin VI isoforms containing NI, the SI, or the SI+LI were found in both the apical and the basolateral regions of MDCK cells (Fig. 2 C), with a very similar localization to that of endogenous myosin VI. In contrast, the full-length myosin VI LI isoform was almost exclusively concentrated at the apical domain, where it showed good colocalization with actin. Thus, this isoform appears to be present in the apical microvilli, which is a region very rich in actin. All the other myosin VI isoforms showed less colocalization with actin at the apical domain, indicating that these isoforms are not recruited into microvilli (Fig. 2 C).

Functional deletion of the myosin VI NI isoform causes missorting of newly synthesized VSV-G

To assess the role of myosin VI in the sorting of newly synthesized proteins from the Golgi complex to the cell surface in

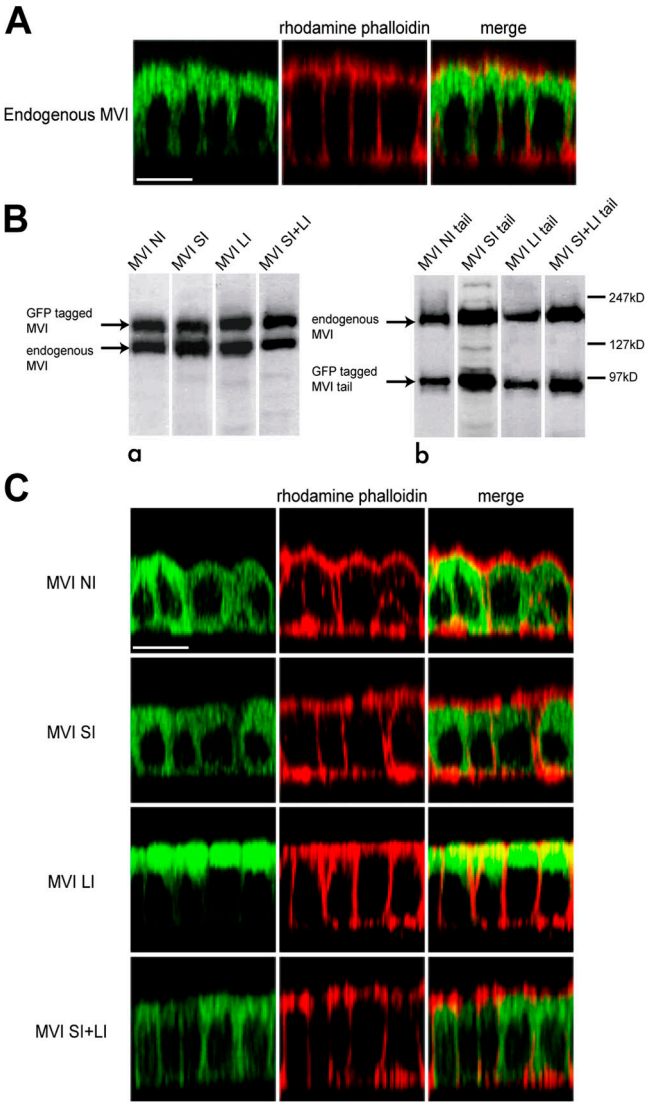

Figure 2. **Localization of myosin VI isoforms in polarized MDCK cells.** (A) Endogenous myosin VI and actin are found at the apical, as well as the basolateral, domain in wild-type MDCK cells. In B, the expression levels of GFP-myosin VI isoforms and GFP-myosin VI tail isoforms are compared by Western blotting to the amount of endogenous myosin VI expressed in stable MDCK cell lines. Note the expression levels of all the expressed GFP-myosin VI and GFP-tails are roughly equal to the amount of endogenous myosin VI. (C) Each myosin VI isoform exhibits a distinct, but overlapping, localization in MDCK cells. (left) Localization of GFP-myosin VI isoforms in MDCK stable cell lines. (middle) Actin distribution stained with rhodamine phalloidin. (right) Merged image of GFP-myosin VI and actin. Bars, 10 μm.

polarized cells, we studied polarized transport in MDCK cells stably expressing the different dominant-negative myosin VI tail isoforms. We used an adenovirus delivery system to express basolateral or apical reporter proteins in these cells. First, we examined the biosynthetic delivery of VSV-G, which is a basolateral membrane protein that is sorted by its cytoplasmic tyrosine motif in an AP-1B–dependent manner. This protein has been used as a reporter molecule for basolateral sorting in numerous studies (Thomas et al., 1993; Folsch et al., 2001, 2003). We monitored the surface appearance of VSV-G using pulse-chase radioactive labeling and domain-selective biotinylation

(Fig. 3). In these experiments, the MDCK cells were grown on filters for 4 d to full polarization, and then pulse labeled with [^{35}S]methionine for 20 min before chasing for the indicated times. At each time point, cells were biotinylated at the apical and basolateral surfaces to measure the amount of reporter protein that had reached each plasma membrane domain.

In control wild-type MDCK cells, cells radiolabeled with VSV-G appeared at the cell surface as early as 30 min into chase, which is consistent with previous studies. At all time points (throughout the entire chase period), 90% of the biotinylated protein was detected on the basolateral surface (Fig. 3 A). In MDCK cells expressing the dominant-negative tail domain containing NI, however, >80% of the biotinylated VSV-G was found on the apical surface throughout the chase (Fig. 3 B). After 30 min of chase, a very small amount (<20%) of the VSV-G appeared at the basolateral surface and disappeared over time. This suggests that the VSV-G may be indirectly missorted using a transcytosis step via the basolateral domain. However, after 30 min, the bulk of the labeled VSV-G is clearly at the apical domain, suggesting direct delivery to the apical surface. Furthermore, recent studies have confirmed that, in MDCK cells, newly synthesized membrane proteins are transported directly to the apical or basolateral surface, i.e., not along a transcytotic route (Hua et al., 2006; Paladino et al., 2006). The fraction of VSV-G reaching the cell surface was ~35% of the total newly synthesized protein in wild-type cells and ~18% in NI tail–expressing cells (Fig. S1, available at http://www.jcb.org/cgi/content/full/jcb.200608126/DC1). This reduction of ~50% in surface delivery of VSV-G was only observed in cells expressing the NI tail and not in cells expressing the other tail isoforms. The dominant-negative effect of the NI tail on the rate of exocytosis is in agreement with our earlier results with Snell's waltzer fibroblasts, which show a 40% reduction in the rate of secreted alkaline phosphatase secretion (Warner et al., 2003). Furthermore, in RNAi experiments, reduced expression levels of myosin VI and optineurin lead to a reduced level of delivery of VSV-G to the cell surface in HeLa cells (Sahlender et al., 2005; unpublished data). In MDCK cells expressing the SI, the LI, or the SI+LI tail, VSV-G was targeted correctly because >80% of the total cell surface biotinylated protein was detected on the basolateral plasma membrane (Fig. 3, C–E). These results suggest that myosin VI is involved in the basolateral sorting of VSV-G, and that it is specifically the NI isoform that carries out this function.

Myosin VI is not involved in sorting to the apical domain in MDCK cells

To establish whether myosin VI is also required for sorting of proteins destined for the apical domain, we examined the polarized delivery of newly synthesized influenza HA. In control

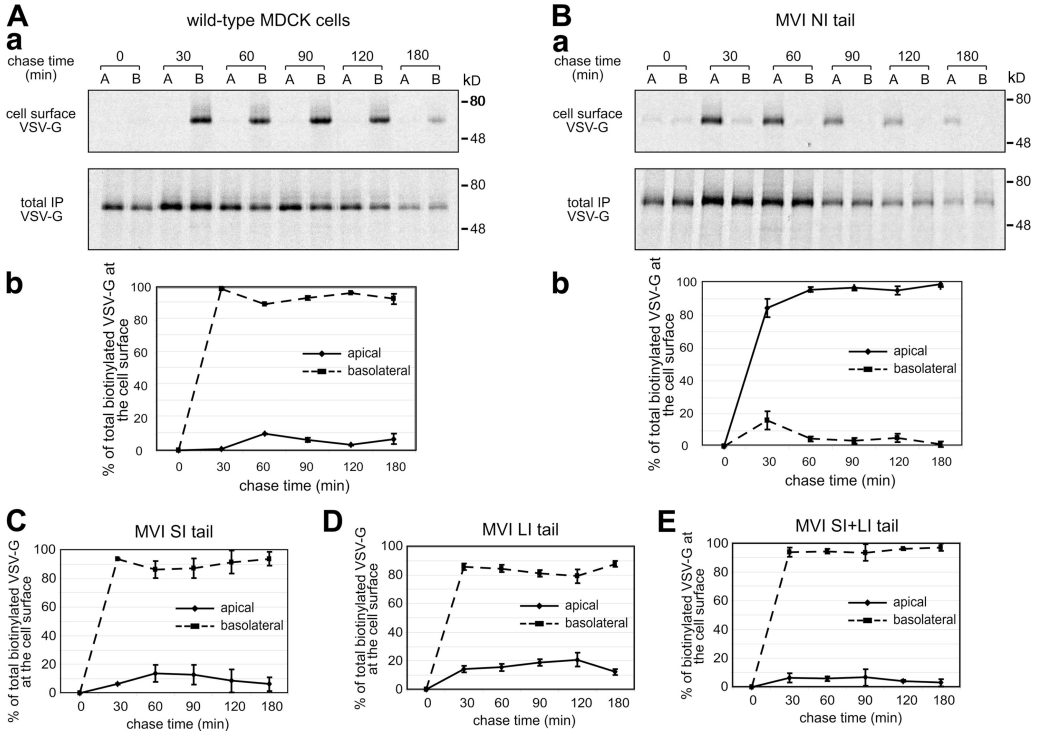

Figure 3. **Expression of the myosin VI tail NI isoform missorts VSV-G to the apical domain in MDCK cells.** (A) In wild-type MDCK cells, VSV-G is sorted and transported to the basolateral domain. Fully polarized MDCK cells were infected for 18 h with VSV-G, and the next day they were pulse labeled with [^{35}S]methionine for 20 min before chasing for 30, 60, 90, 120, and 180 min. At each time point, the apical and the basolateral surfaces were biotinylated and the total VSV-G was immunoprecipitated. From this pool, the biotinylated VSV-G was precipitated using streptavidin beads. (a) The autoradiography of apical (A) VSV-G, basolateral (B) VSV-G, and total immunoprecipitated (IP) VSV-G in wild-type MDCK cells. (b) Graphical representation of the percentage of total biotinylated VSV-G reaching the apical (solid line) or the basolateral (dashed line) cell surface. (B) VSV-G is missorted to the apical surface in MDCK cells overexpressing the myosin VI NI tail. (C–E) VSV-G is sorted normally to the basolateral domain in MDCK cells overexpressing the myosin VI tail with SI, LI, or SI+LI.

wild-type MDCK cells, >90% of the HA reaching the cell surface was found on the apical plasma membrane after 1 and 2 h of chase (Fig. 4 A). Consistent with previous studies, HA is transported directly from the TGN to the apical surface without passing through the basolateral surface (Lin et al., 1998; Tall et al., 2003). In MDCK cells expressing the four different myosin VI tail isoforms after 2 h of chase, >90% of the cell surface HA was also found at the apical plasma membrane (Fig. 3, B–E); i.e., no mistargeting to the basolateral domain was observed. These observations suggest that none of the myosin VI isoforms are involved in HA sorting to the apical domain in MDCK cells.

The detailed mechanisms involved in the apical sorting pathways are still poorly understood. However, there are at least three different groups of apical sorting determinants that reside either in the extracellular, transmembrane, or cytoplasmic domains of the cargo proteins, and they probably use different pathways. The sorting signal of HA is located in its transmembrane domain, which also mediates lipid raft association (Lin et al., 1998; Shvartsman et al., 2003). To confirm that myosin VI was not required for sorting of apical proteins with different sorting signals, we also examined the trafficking of endolyn and an endolyn–megalin chimera. The sialomucin endolyn contains N-glycan–dependent apical targeting information in its ectodomain. This protein has a lysosomal steady-state localization in many cell types that is caused by the interaction of its cytoplasmic YxxΦ motif with AP-3; however, this motif binds only weakly to other AP complexes and is recessive to the apical sorting signal for polarized surface delivery (Ihrke et al., 2001, 2004). Megalin is sorted apically by a peptide motif present in its cytoplasmic tail (Marzolo et al., 2003; Takeda et al., 2003). Therefore, we fused this megalin tail to the ecto- and transmembrane domain of endolyn and used this chimera as the third apical reporter. The results obtained with these two additional marker proteins in MDCK cells expressing any of the different tail isoforms, were very similar to those observed for HA (unpublished data). In addition, the endogenous apical protein gp135 shows a normal immunofluorescence distribution under all conditions in these MDCK cells (Fig. 6 C), which further confirms that myosin VI is not involved in the sorting of proteins to the apical domain of polarized MDCK cells.

Functional deletion of the myosin VI NI isoform missorts only AP-1B–dependent basolateral cargo

To establish whether the myosin VI NI isoform affects only the sorting of specific basolateral cargo, we compared the cell surface targeting of AP-1B–dependent and -independent reporter molecules by indirect immunofluorescence. VSV-G and the LDL receptor both contain a tyrosine motif and use the AP-1B–dependent

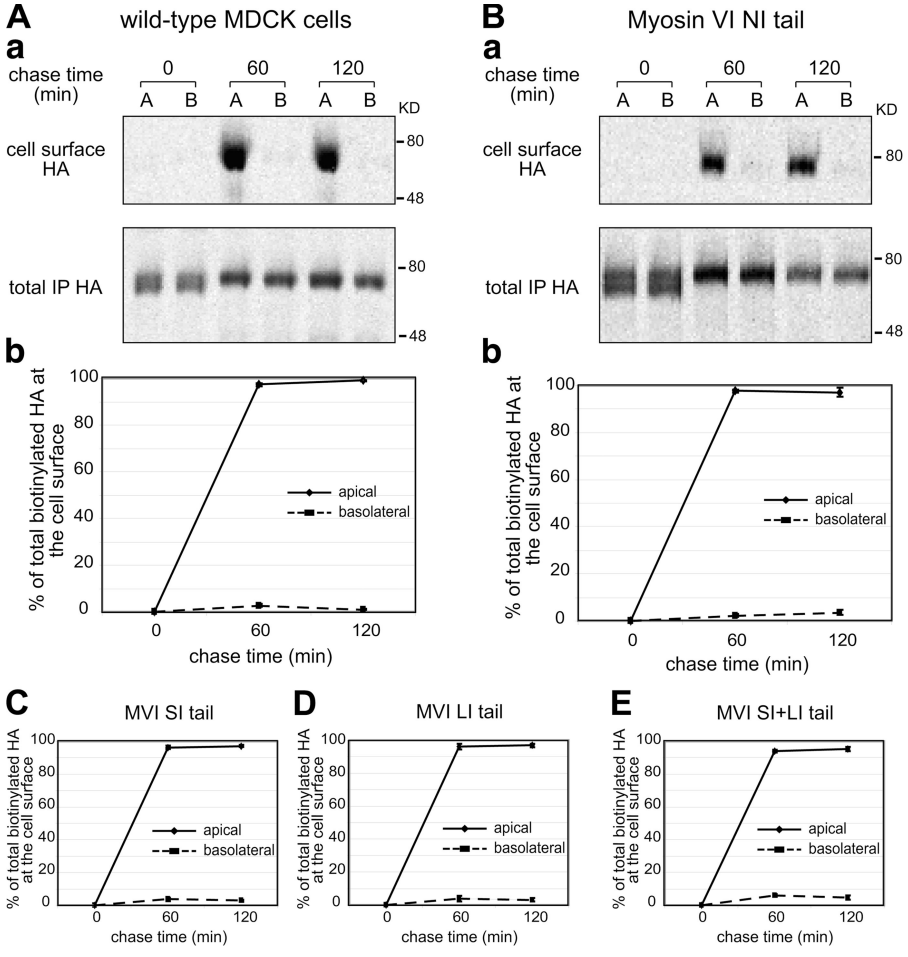

Figure 4. **Myosin VI is not involved in sorting of HA to the apical domain in MDCK cells.** (A) In wild-type MDCK cells, HA is sorted and transported to the apical domain. (a) The autoradiography of apical (A) HA, basolateral (B) HA, and total immunoprecipitated (IP) HA. (b) Graphical representation of the percentage of total biotinylated HA that has reached either the apical (solid line) or the basolateral (dashed line) cell surface. (B) HA is correctly sorted to the apical surface in MDCK cells overexpressing the myosin VI NI tail. C–E are also sorted normally to the apical domain in MDCK cells overexpressing the myosin VI tail with SI, LI, or SI+LI.

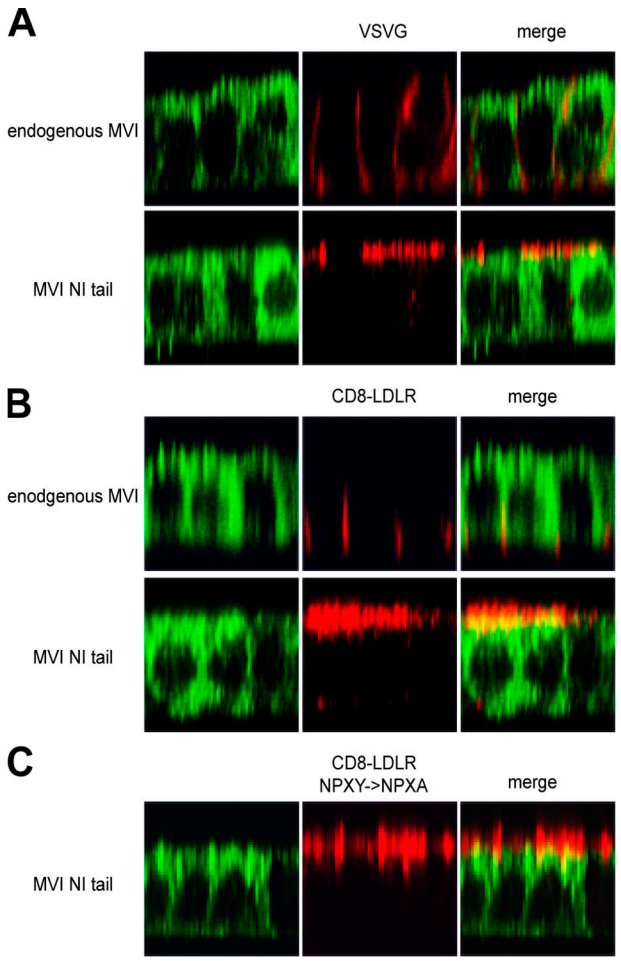

Figure 5. **Expression of the myosin VI NI tail isoform results in missorting of AP-1B–dependent cargo in MDCK cells.** In A and B, the immunofluorescent localization of VSV-G and CD8-LDLR in wild-type MDCK cells and MDCK cells expressing the myosin VI NI tail are shown. In C, the localization of CD8-LDLR containing a mutation in the NPXY endocytosis signal (NPXY–NPXA) in MDCK cells expressing myosin VI NI tail is shown. VSV-G and the LDLR are AP-1B–dependent cargos that are sorted to the basolateral domain in wild-type MDCK cells, but are localized at the apical domain in cells overexpressing the myosin VI NI tail. The endocytosis-defective CD8-LDLR is directly mistargeted to the apical domain, and no transcytosis step after endocytosis at the basolateral domain is involved. MDCK cells were infected with the virus encoding tsO45 VSV-G and incubated at 40°C overnight to accumulate VSV-G in the ER before a 2-h chase at 31°C in the presence of cycloheximide allowed the VSV-G to exit and accumulate on the cell surface. Cells infected with CD8-LDLR were incubated in the presence of cyclohexamide at 20°C for 3 h to accumulate the protein in the Golgi before release at 37°C. Cells were fixed without permeabilization and stained for cell surface VSV-G using an antibody to the luminal domain of VSV-G or with an antibody to CD8 to detect the CD8-LDLR chimera. The cells were permeabilized and stained for endogenous myosin VI in wild-type MDCK cells and for GFP in cells overexpressing myosin VI NI tail. Confocal vertical X–Z optical sections are shown. Bar, 10 μm.

basolateral sorting pathway (Folsch et al., 1999; Sugimoto et al., 2002). To monitor LDL receptor uptake we used a CD8-LDL receptor chimera containing the extracellular and transmembrane domains of CD8 fused to the LDL receptor tail (Motley et al., 2003). Basolateral targeting of the immunoglobulin Fc receptor (FcγRIIB), however, depends on a dileucine motif, which directs the receptor into an AP-1B–independent pathway to the basolateral domain (Roush et al., 1998; Folsch et al., 1999).

In the first experiment, we used VSV-G, which we have shown in the cell surface biotinylation assay to be missorted to the apical domain in cells expressing the dominant-negative myosin VI NI tail. The VSV-G used is the temperature-sensitive mutant (tsO45 VSV-G; Gallione and Rose, 1985), which accumulates in the ER at 40°C, the nonpermissive temperature. Lowering the temperature to 31°C allows the protein to fold and to be transported to the cell surfaces via the Golgi complex. Therefore, after infection with the virus encoding tsO45 VSV-G, the cells were first grown at 40°C to accumulate the protein in the ER before shifting to the permissive temperature in the presence of cycloheximide to initiate synchronous transport of VSV-G through the Golgi to the cell surface. VSV-G present on the cell surface of nonpermeabilized cells was recognized by an antibody against the luminal domain of VSV-G (Pepperkok et al., 1993). VSV-G was mainly present on the basolateral surface in wild-type MDCK cells, as shown in Fig. 5 A. In contrast, expression of the myosin VI tail isoform with NI resulted in the apical appearance of VSV-G (Fig. 5 A). Expression of myosin VI tail isoforms with the SI, the LI, or the SI+LI exhibited a subcellular localization similar to wild-type MDCK cells (unpublished data). Thus, these VSV-G immunofluorescent localization data are in good agreement with the results of the domain-selective biotinylation (Fig. 3).

The other two reporter proteins we used, the CD8-LDL receptor tail chimera and FcγRIIB, are not temperature-sensitive mutants, and therefore a different temperature-shift protocol was used to synchronize these proteins. After infection with virus encoding these proteins and overnight incubation, the cells were incubated at 20°C for 3 h in the presence of cycloheximide to accumulate the proteins in the Golgi before raising the temperature to 37°C to release the proteins from the Golgi to the cell surface.

As observed with VSV-G, the CD8-LDL receptor tail chimera was missorted to the apical surface in cells expressing the myosin VI dominant-negative NI tail (Fig. 5 B), whereas it was sorted correctly to the basolateral surface in wild-type MDCK cells (Fig. 5 B) and in cells expressing myosin VI tails with the SI, the LI, or the SI+LI (not depicted). To address the question of whether apical missorting of the CD8-LDL receptor involves transcytosis, we expressed an endocytosis-defective LDL receptor construct with a mutation in the endocytosis signal (NPXY–NPXA) in myosin VI NI tail–expressing cells (Chen et al., 1990). Like the wild-type CD8-LDL receptor, the mutant receptor is delivered to the apical domain (Fig. 5 C). This result clearly indicates that in myosin VI NI tail–expressing cells AP-1–dependent cargo is missorted directly to the apical domain and does not involve endocytosis and transcytosis via the basolateral domain.

In striking contrast to these observations, the FcγRIIB receptor (containing a dileucine sorting motif) was targeted correctly to the basolateral surface in cells expressing the myosin VI NI tail (Fig. 6 A) and in cells expressing the other myosin VI tails (not depicted). These results suggest that the myosin VI NI isoform is specifically responsible for the sorting of AP-1B–dependent cargos to the basolateral plasma membrane in polarized MDCK cells. Further support for these results is provided by

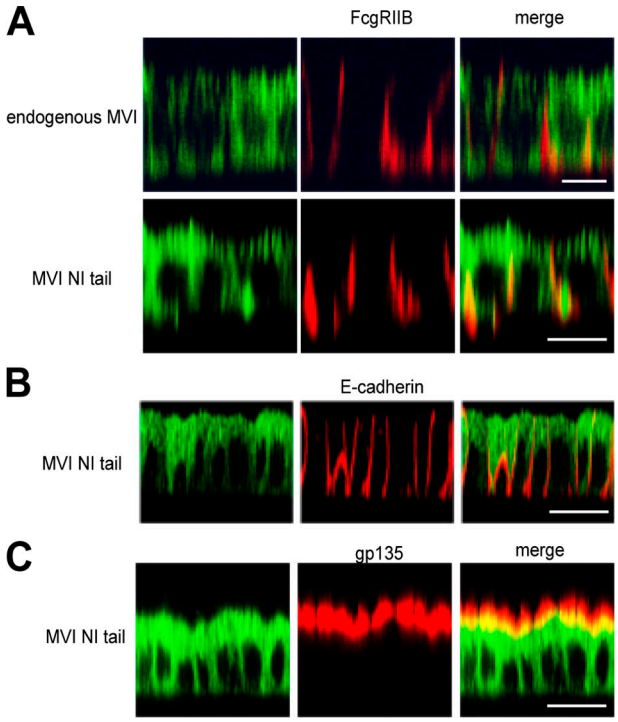

Figure 6. **Expression of the myosin VI NI tail has no affect on FcγRIIB sorting or the localization of E-cadherin and gp135 in MDCK cells.** FcγRIIB is sorted and transported correctly to the basolateral domain in both wild-type and myosin VI NI tail–expressing cells. (A, left) The localization of endogenous myosin VI in wild-type MDCK cells or in cells expressing GFP-myosin VI NI tail. (A, middle) The distribution of FcγRIIB in the cells. (A, right) Merged images. MDCK cells were infected overnight with virus encoding FcγRIIB, and then incubated at 20°C to accumulate the protein in the Golgi for 2 h, before a chase at 37°C in the presence of cycloheximide. Cells were fixed and stained for the FcγRIIB on the cell surface before permeabilization and staining for endogenous myosin VI in wild-type MDCK cells or for GFP in cells expressing GFP-myosin VI NI tail. MDCK cells expressing the myosin VI NI tail show normal steady-state distribution of the basolateral marker E-cadherin (B) and the apical marker protein gp135 (C). (left) The localization of the GFP-myosin VI NI tail. (middle) Transfected cells stained with antibodies either to E-cadherin or gp135. (right) Merged image of the corresponding left and middle images. Confocal vertical X–Z optical sections are shown. Bars, 10 μm.

the observation that the steady-state distribution of endogenous E-cadherin, whose basolateral sorting also depends on a dileucine motif, is unchanged in cells expressing the myosin VI NI tail (Fig. 6 B) or the other myosin VI tail isoforms (not depicted).

A myosin VI–optineurin complex functions in the AP-1B basolateral protein sorting pathway

Recently, several components involved in AP-1B–dependent basolateral protein sorting, such as the small GTPase Rab8, have been identified. Expression of a constitutively active Rab8 missorts VSV-G and LDL receptors, but not FcγRIIB, to the apical surface in MDCK cells, and overexpression of Rab8 causes disruption of AP-1 localization (Ang et al., 2003). As Rab8 interacts with the myosin VI binding partner, optineurin (Hattula and Peranen, 2000; Sahlender et al., 2005), we next asked if optineurin might link myosin VI to Rab8 in the AP-1B–dependent sorting pathway. Because we previously

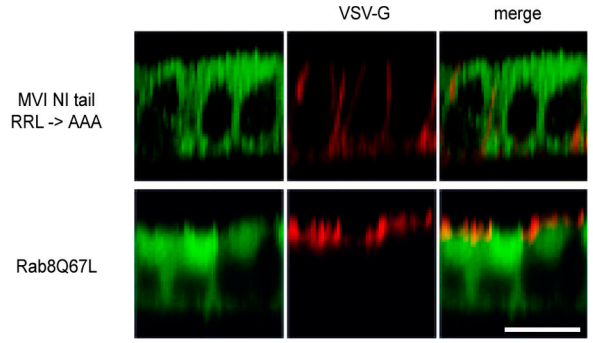

Figure 7. **When the optineurin binding site in the myosin VI NI tail is mutated, VSV-G is not missorted to the apical domain.** In MDCK cells expressing the myosin VI NI tail with the RRL–AAA mutation, VSV-G is sorted normally to the basolateral domain, whereas in the MDCK cells expressing the constitutively active GFP-Rab 8 Q67L, VSV-G is missorted to the apical domain. Stable MDCK cell lines expressing either mutant GFP-myosin VI NI tail, RRL–AAA or constitutively active GFP-Rab8-Q67L were grown on filters and fully polarized before infecting with the virus encoding tsO45 VSV-G. The infected cells were incubated at 40°C overnight to accumulate VSV-G in the ER, before a 2-h chase at 31°C in the presence of cycloheximide. Cells were fixed without permeabilization and stained for cell surface VSV-G using an antibody to the luminal domain of VSV-G. After permeabilization, GFP-tagged NI mutant tail or Rab8Q67L were detected with an antibody to GFP. (right) The merged image of the corresponding left and middle images. Confocal vertical X–Z optical sections are shown. Bar, 13 μm.

identified the optineurin binding site (RRL; aa 1,107–1,109) in the C-terminal globular tail domain of myosin VI, we mutated this binding motif to three alanines (RRL–AAA) in the NI tail isoform and generated stable cell lines expressing this mutant NI tail. We also established stable cell lines expressing the constitutively active form of Rab8 (Rab8-Q67L). Expression of Rab8-Q67L and the wild-type myosin VI NI tail resulted in indistinguishable phenotypes, with VSV-G being missorted to the apical surface (Fig. 7; Ang et al., 2003). In cells overexpressing the myosin VI NI tail, no change in AP-1 localization was observed (Fig. S2, available at http://www.jcb.org/cgi/content/full/jcb.200608126/DC1; Ang et al., 2003). However, in cells expressing the myosin VI NI tail with the mutated optineurin binding site, VSV-G was correctly transported to the basolateral surface (Fig. 7). These results, together with previous data, strongly suggest that myosin VI, optineurin, and Rab8 operate in the same basolateral sorting pathway and, most likely, form a functional complex.

Myosin VI colocalizes with AP-1 in endosomes

It is still a matter of debate whether AP-1B–dependent sorting occurs at the TGN or in a post-TGN compartment, such as recycling endosomes. Therefore, we determined the localization of myosin VI and optineurin at the EM level in polarized MDCK cells. In nonpolarized fibroblasts, myosin VI has previously been shown, at the ultrastructural level, to be associated with vesicles at the trans side of the Golgi complex and with clathrin-coated structures at the plasma membrane (Buss et al., 2001; Warner et al., 2003). In polarized MDCK cells, we observed that myosin VI and optineurin colocalize with AP-1 on clathrin-coated endosomes and clathrin-coated vesicles surrounding

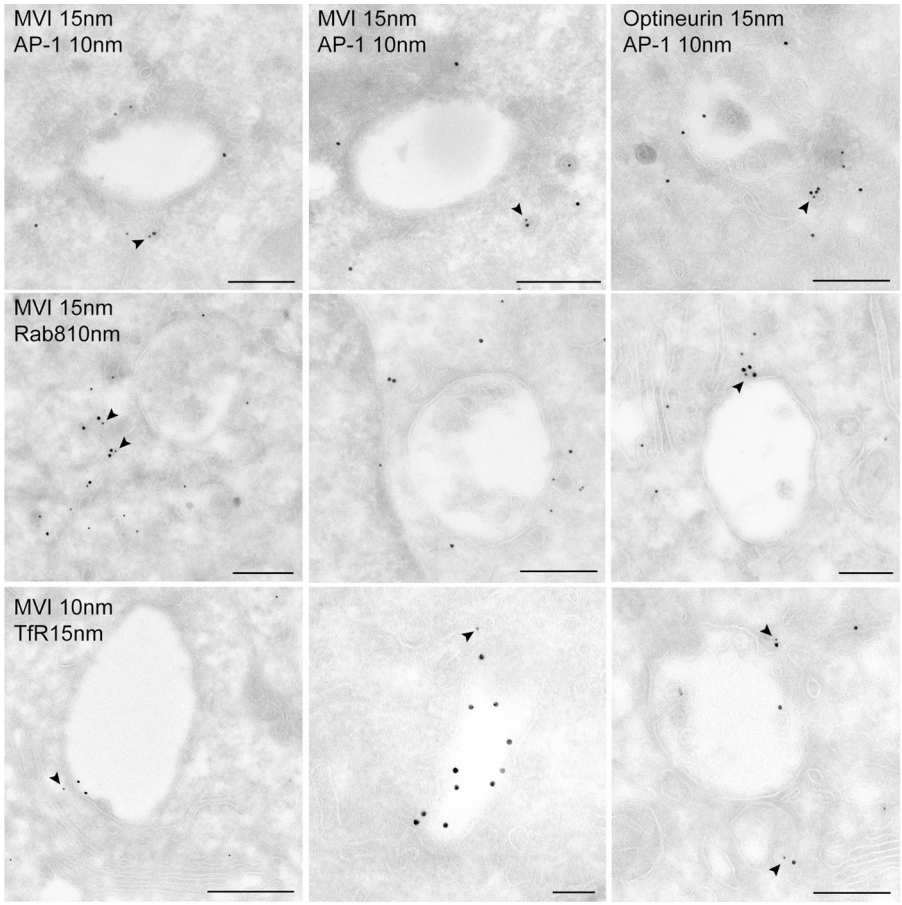

Figure 8. **Myosin VI and optineurin colocalize with AP-1, Rab8, and TfR in recycling endosomes.** Cryosections of polarized MDCK cells were double labeled with antibodies against endogenous AP-1 (10-nm gold) and myosin VI (15-nm gold) or with antibodies against AP-1 (10-nm gold) and optineurin (15-nm gold). Cryosections of polarized MDCK cells stably expressing GFP-Rab8 were labeled with antibodies against endogenous myosin VI (15-nm gold) and with antibodies to GFP for localization of Rab8 (10-nm gold). For further characterization, the human TfR was expressed in MDCK cells and an antibody uptake experiment with a monoclonal antibody to the human TfR was performed. Cryosections of these cells show colocalization of endogenous myosin VI (10-nm gold) and TfR (15-nm gold) in recycling endosomes. Myosin VI and optineurin are present on AP-1–, Rab8-, and TfR-positive recycling endosomes and small clathrin–coated vesicles surrounding these endosomes. Arrowheads show colocalization of myosin VI or optineurin with AP-1, Rab8, or TfR. Bars, 450 nm.

these endosomes (Fig. 8). To further characterize these endosomes, we raised a stable MDCK cell line expressing GFP-Rab8. We performed double-labeling experiments on cryosections with antibodies to GFP to label Rab8 and with antibodies to myosin VI to visualize the endogenous protein. Finally, we expressed the human TfR in MDCK cells and performed an antibody uptake experiment from the basolateral domain with a monoclonal antibody to the human TfR to localize the endocytosed receptor. Endogenous myosin VI can be found in recycling endosomes colocalizing with the TfR and with Rab8. Collectively, these results show that myosin VI and optineurin are present in Rab8- and TfR-positive recycling endosomes, where they colocalize with AP-1 and may function in the sorting of cargo to the basolateral domain.

Discussion

Compelling evidence is presented that myosin VI is an essential component of the basolateral sorting machinery in the AP-1B–dependent pathway in polarized epithelial cells. Although three different splice variants of myosin VI are expressed in polarized MDCK cells, only the isoform with NI in the tail domain is required for correct sorting of specific membrane proteins to the basolateral domain. Interestingly, none of the myosin VI isoforms is required for the sorting of proteins to the apical domain. Expression of the dominant-negative myosin VI NI tail mutant selectively results in missorting of plasma membrane proteins containing tyrosine-based sorting motifs that interact with the clathrin adaptor complex AP-1B. These results add myosin VI to the growing list of components, such as Rab8 and cdc42, which are essential for the AP-1B–dependent basolateral sorting pathway.

The Rho family GTPase cdc42 is a key regulator of the actin cytoskeleton, and the effects caused by overexpression of constitutively active or inactive cdc42 mutants highlights the importance of actin polymerization/depolymerization for basolateral sorting (Kroschewski et al., 1999; Musch et al., 2001; Sheff et al., 2002). Although the exact role of actin filaments in vesicle transport to the basolateral domain is not known, it is likely that one function is to provide tracks for myosin VI–based movement to exert pulling, tethering, or transport forces on exocytic membranes and vesicles. Using the myosin toxin BDM, which is now believed to solely inhibit myosin II activity (Ostap, 2002), it has been shown that the release of basolateral transport vesicles from the Golgi complex in MDCK cells is prevented (Musch et al., 1997). Thus, inhibition of myosin II activity, which stabilizes the actin filament network surrounding the Golgi complex, appears to lead indirectly to inhibition of basolateral transport. In contrast, the role of myosin VI in basolateral sorting appears to be directly related to the formation of a functional sorting complex.

Interestingly, our previous work in nonpolarized cells demonstrated that optineurin links myosin VI to Rab8, and all three proteins are present in the perinuclear region at/around

the Golgi complex and on vesicles close to the plasma membrane (Sahlender et al., 2005). In nonpolarized cells, overexpressing a constitutively active Rab8 mutant causes the production of long, tubular membrane structures emerging from the perinuclear region. Myosin VI is specifically recruited to these structures, indicating that GTP-bound Rab8 may serve as a membrane anchor for myosin VI (Sahlender et al., 2005). It is believed that one function of Rab proteins is to serve as molecular tags on the cytoplasmic surface of membrane compartments to mediate recruitment of cytosolic components such as, for example, actin-based and microtubule-based motor proteins (Zerial and McBride, 2001). Therefore, Rab8 may recruit myosin VI to the AP-1B sorting compartment via optineurin. Further support for this idea is provided by the observation that mutation of the optineurin binding site on myosin VI ablates the negative inhibitory effect of the myosin VI tail domain NI isoform on basolateral sorting. These results suggest that a functional complex between myosin VI, optineurin, and Rab8 plays a crucial role in the AP-1B–dependent sorting pathway. But at which step along the AP-1B–dependent sorting pathway does myosin VI function? In our previous studies in nonpolarized cells, we localized myosin VI in vesicles at the trans side of the Golgi complex that were, on average, 200–500 nm away from TGN38, which is a marker protein for the trans-Golgi network (Warner et al., 2003). Interestingly, this distribution of myosin VI on vesicles near the TGN is very similar to the reported localization of the AP-1B–positive compartment (~500 nm away from Golgi cisternae; Folsch et al., 2001, 2003). In this study, we show that in polarized MDCK cells myosin VI and optineurin colocalize with AP-1 on clathrin-coated endosomal structures, which are most likely recycling endosomes based on the colocalization of myosin VI with TfR and Rab8 in similar structures. Recently, it has been demonstrated that recycling endosomes play an important role in basolateral sorting and contain components of the AP-1B–dependent pathway, such as Rab8 and exocyst subunits involved in the basolateral sorting pathway (Ang et al., 2004). At the recycling endosome, myosin VI could initially be involved in segregating/clustering AP-1B–dependent basolateral cargo into clathrin-coated subdomains. Subsequently, myosin VI could facilitate the formation of a clathrin-coated transport vesicle by pulling membrane away from the endosome, and therefore supporting vesicle scission. Finally, it could transport the cargo vesicle formed over short distances toward the basolateral domain. The orientation of actin filaments around endosomes is currently unknown; however, studies from isolated phagosomes indicate (Defacque et al., 2000) that the plus-ends of actin filaments are directed toward the surface of phagosomes. Therefore, the minus end directionality of myosin VI favors the pulling of membrane away from the endosomal surface and the movement of vesicles away from the endosome.

In nonpolarized cells, we have shown (Sahlender et al., 2005) that myosin VI, optineurin, and Rab8 colocalize in vesicles underneath the plasma membrane. These results suggest that myosin VI, in conjunction with Rab8, might be required for the delivery of basolateral cargo to the plasma membrane, where it might cooperate with the exocyst complex in the tethering of vesicles before fusion. In yeast, the Rab8 homologue Sec4p targets vesicles to sites of exocytosis at the cell surface (Guo et al., 1999). In mammalian cells, the exocyst complex is only required for basolateral, but not for apical, delivery of cargo (Grindstaff et al., 1998). Interestingly, like myosin VI, subunits of the exocyst complex can be found both at the plasma membrane and in the perinuclear area, probably in the recycling endosome (Folsch et al., 2003).

So how are basolateral cargoes missorted to the apical domain when myosin VI function is blocked? If only myosin VI–driven transport of AP-1B–specific basolateral carriers along actin filaments was inhibited, it would lead to an accumulation of secretory vesicles in the perinuclear area or around recycling endosomes, but would not result in apical mistargeting. In addition, loss of myosin VI function in exocyst-mediated tethering of AP-1B–specific vesicles to the basolateral domain would also not necessarily result in apical missorting of basolateral proteins; instead, one would expect a nonpolarized distribution of these vesicles. Thus, it appears that myosin VI is involved in cargo sorting or vesicle formation at the donor compartment, and when this function is inhibited, it results in the incorporation of basolateral membrane proteins into apical carriers and their delivery to the apical domain.

Why is only the NI isoform of myosin VI involved in basolateral sorting, when both the LI and the SI+LI myosin VI isoforms are also expressed in polarized MDCK cells? Our PCR results indicate that the NI and LI are the major isoforms expressed in polarized MDCK cells, and that the SI+LI is only expressed to a lesser extent. The data showing the localization of the different myosin VI isoforms (Fig. 2) indicate that the isoform containing the LI is specifically targeted to the apical domain and is not present in the perinuclear area where basolateral sorting, either in the TGN or the recycling endosome, occurs. The LI enhances targeting of myosin VI to clathrin-coated structures via Dab2 (Morris et al., 2002); therefore, this isoform is believed to play a role in clathrin-mediated endocytosis at the apical domain of polarized epithelial cells (Buss et al., 2001). Thus, differential intracellular targeting appears to be an important mechanism for regulating the intracellular functions of the different myosin VI splice variants expressed together in a single cell type. It is not clear what "advantage" the absence of the SI and LI inserts in the tail confers on myosin VI in respect to basolateral protein sorting. The SI and LI inserts do not contain any obvious structural motifs or apparent binding or regulatory sites. However, these inserts are located in or next to the C-terminal "cargo-binding" tail domain, which is responsible for the cellular targeting of myosin VI, and thus may have an effect on the conformation of the tail domain, and possibly on the whole molecule. In accordance with this hypothesis, recent studies have shown that the cargo-binding C-terminal tail domain of myosin Va interacts with the motor "head" domain regulating myosin Va motor activity (Wang et al. 2004; Liu et al., 2006; Thirumurugan et al., 2006). Thus, structural, functional, and single-molecule imaging studies are underway to determine the importance of the inserts (or their absence) on the regulation and function of myosin VI.

In conclusion, we have demonstrated that in polarized epithelial cells, myosin VI is important for sorting and basolateral delivery of newly synthesized membrane proteins that use the AP-1B–dependent pathway. However, the exact cellular locations, the mechanistic details, and whether, for example, the myosin VI NI isoform operates as a nonprocessive monomer or processive dimer, its precise interacting components, and the regulatory signals used are just a few of the unknowns that need to be determined.

Materials and methods

Antibodies
The affinity-purified rabbit polyclonal antibodies to the whole tail (α-MVI), globular tail of myosin VI (α-MVI-GT), human full-length optineurin (Buss et al., 1998; Warner et al., 2003: Sahlender et al., 2005), and mouse monoclonal antibody to rat endolyn (501; Ihrke et al., 1998) have been previously described. The mouse monoclonal antibody to human CD8 was obtained from M. Seaman (Cambridge Institute for Medical Research [CIMR], Cambridge, UK); the mouse monoclonal anti-HA Fc125 tissue culture supernatant was obtained from O. Weisz (University of Pittsburgh, Pittsburgh, PA); the mouse monoclonal antibody to the luminal domain of VSV-G was obtained from R. Pepperkok and J. Simpson (European Molecular Biology Laboratory, Heidelberg, Germany); and the rabbit polyclonal antibody to AP-1 was obtained from M. Robinson (CIMR, Cambridge, UK). The following commercial antibodies were used: a mouse monoclonal antibody to GFP (Abcam), a rabbit polyclonal antibody to GFP (Abcam), rabbit anti–mouse (DakoCytomation), protein A gold (Cell Microscopy Centre, Utrecht, Netherlands), a mouse monoclonal antibody to human CD32/FcγRII (R&D Systems), a mouse monoclonal antibody to E-cadherin (Developmental Studies Hybridoma Bank, Iowa City, Iowa), a mouse monoclonal antibody to VSV-G (Sigma-Aldrich), and a mouse monoclonal antibody to human TfR (5E9C11; American Type Culture Collection).

PCR analysis
RT-PCR analysis was used to assess the expression of myosin VI isoforms in nonpolarized MDCK cells grown on plastic and in polarized MDCK cells grown on transwell filters, as described in Buss et al. (2001).

pShuttle constructs
The cDNAs of endolyn (Ihrke et al., 2000), CD8-LDLR (a gift from M. Seaman), HA (a gift from O. Weisz), FcγRIIB (a gift from A. Floto, CIMR, Cambridge, UK), VSV-G tsO45 (a gift from R. Duden, University of London, London, UK), and human TfR were amplified by PCR and inserted into the pShuttle-CMV vector (Stratagene) for preparing recombinant adenoviruses.

Recombinant adenoviruses and infection
Recombinant adenoviruses were produced using the AdEasy Adenoviral vector system (Stratagene) and used to infect filter-grown MDCK cells. MDCK cells grown for 3 d on filters were washed twice with PBS++ (PBS supplemented with 0.9 mM $CaCl_2$, 0.52 mM $MgCl_2$, and 0.16 mM $MgSO_4$) before adding 10 plaque-forming units/cell of purified recombinant viruses diluted in PBS++ (50 μl for 6.5 mm filters; 200 μl for 12 mm filters) to the apical compartment, while the basolateral compartment was incubated with only PBS++ (600 μl for 6.5-mm filters; 1.5 ml for 12-mm filters). After 1.5 h at 37°C, the virus-containing medium was replaced with normal growth medium, and the cells were incubated for an additional 18 h before performing the biochemical assays.

Cell culture
MDCK II cells were cultured at 37°C under 5% CO_2 in D-MEM (Invitrogen) containing 10% (vol/vol) fetal calf serum (HyClone), 100 U/ml penicillin, and 0.1 mg/ml streptomycin (Invitrogen). The cells were plated at 10^5 cells/cm^2 on 0.4 μm polycarbonate membrane Transwell filters (Corning Costar) and grown for 4 d with a daily medium change. Cell polarization was monitored by measuring the transepithelial electrical resistance using a Mitchell-ERS epithelial voltameter (Millipore).

Stable transfection and selection of MDCK cells
Myosin VI, the tail domains, or full-length Rab8 tagged with GFP at the N-terminus were cloned into the ΔpMEP4 vector, which controls protein expression by the inducible metallothionein IIA promotor. Protein expression was induced for 24 h with 100 μM $ZnCl_2$. To generate stable MDCK cell lines, transfected cells were selected with 200 μg/ml Hygromycin (Roche). Single clones were isolated, and expression of the various myosin VI isoforms was checked by immunofluorescence and immunoblotting with an antibody to the myosin VI tail. The four best individual clones for each construct were grown in selective medium and the population of highly expressing cells enriched by FACS sorting.

Immunofluorescence microscopy
Indirect immunofluorescence staining was performed as described in Ihrke et al. (2001). For TfR antibody uptake experiments, MDCK cells were infected with virus containing human TfR overnight, serum starved for 1 h, and incubated for 30 min in the basolateral compartment with the monoclonal antibody to TfR, before fixation and processing for EM. For cell surface staining of VSV-G, infected MDCK cells were incubated at 39.5°C overnight to accumulate VSV-G in the ER, followed by 31°C for 2 h in the presence of 100 μg/ml cycloheximide (Sigma-Aldrich). MDCK cells expressing either the CD8-LDLR chimera or the FcγRIIB were incubated at 37°C overnight, followed by a 20°C block for 3 h to accumulate proteins in the Golgi complex in the presence of cycloheximide before a temperature shift to 37°C enables protein exit from the Golgi complex to the cell surface. To visualize proteins on the cell surface the cells were fixed and before permeabilization incubated with antibodies recognizing the luminal domain of VSV-G, CD8, or the FcγRIIB. Cells were visualized in a Radiance Plus confocal scanning microscope with a 63×/NA 1.4 objective at a resolution of 1,024 × 1,024 pixels (Bio-Rad Laboratories). Photoshop software (Adobe) was used for image processing.

Immunoelectron microscopy
Polarized MDCK II cells were fixed in a mixture of 2% paraformaldehyde and 0.2% glutaraldehyde in PBS for 2 h. The cells were washed with PBS containing 0.02 M glycine to quench aldehydes, scraped off the filter, centrifuged, and embedded in 12% gelatin in PBS. Small blocks of embedded cells were incubated overnight with 2.3 M sucrose at 4°C, mounted on aluminum pins, and frozen in liquid nitrogen. Ultrathin 70-nm cryosections were cut at −120°C and picked up with a mixture of 1% methylcellulose in 1.15 M sucrose. The sections were processed for labeling using previously described protocols (Puri et al., 2005).

Pulse-chase labeling and cell surface biotinylation
For ^{35}S labeling, MDCK cells grown on transwell filters were starved for 30 min in Met-/Cys-free MEM (Sigma-Aldrich) containing 10% dialyzed FCS (Sigma-Aldrich), radiolabeled for 20 min with 0.1 mCi Redivue PRO-MIX (GE Healthcare), and then chased for different times in D-MEM (Invitrogen) supplemented with 5× Met and Cys and 10% FCS. The side of the Transwell to be biotinylated was incubated twice for 20 min with 1.5 mg/ml Sulfo-NHS-Biotin derivatives in 1 ml PBS. The reaction was quenched by addition of 100 mM glycine in PBS. The solubilization and immunoprecipitation procedures are described in Ihrke et al., (2001). Samples were separated by 10% SDS PAGE, and the dried gel was exposed to a phosphorimaging screen for 24 h. The screen was scanned with a Cyclone phosphorimager (Perkin Elmer), and the intensity of the bands was quantitated using OptiQuant software. The percentage of a reporter protein reaching the cell surface relative to the total cell surface biotinylated protein was calculated by dividing the biotinylated protein on that cell surface by the total biotinylated protein. Values are averages from four experiments using two different stable clones and are presented with standard deviations.

Online supplemental material
Fig. S1 shows graphical representations of the amount of VSV-G at the cell surface. Fig. S2 shows that overexpression of GFP-myosin NI tail does not disrupt AP-1 localization in MDCK cells. The online version of this article is available at http://www.jcb.org/cgi/content/full/jcb.200608126/DC1.

We thank Drs. O. Weisz, M. Seaman, R. Duden, A. Floto, R. Pepperkok, J. Simpson, and M. Robinson for the generous gifts of antibodies and cDNAs.

This work was funded by a Wellcome Trust Senior Fellowship (F. Buss) and a Croucher Foundation Research Studentship (J. Au), and was supported by the Medical Research Council. CIMR is in receipt of a strategic award from the Wellcome Trust.

Submitted: 21 August 2006
Accepted: 5 March 2007

References

Ang, A.L., H. Folsch, U.M. Koivisto, M. Pypaert, and I. Mellman. 2003. The Rab8 GTPase selectively regulates AP-1B-dependent basolateral transport in polarized Madin-Darby canine kidney cells. *J. Cell Biol.* 163:339–350.

Ang, A.L., T. Taguchi, S. Francis, H. Folsch, L.J. Murrells, M. Pypaert, G. Warren, and I. Mellman. 2004. Recycling endosomes can serve as intermediates during transport from the Golgi to the plasma membrane of MDCK cells. *J. Cell Biol.* 167:531–543.

Aschenbrenner, L., T. Lee, and T. Hasson. 2003. Myo6 facilitates the translocation of endocytic vesicles from cell peripheries. *Mol. Biol. Cell*. 14:2728–2743.

Buss, F., J. Kendrick-Jones, C. Lionne, A.E. Knight, G.P. Cote, and J. Paul Luzio. 1998. The localization of myosin VI at the Golgi complex and leading edge of fibroblasts and its phosphorylation and recruitment into membrane ruffles of A431 cells after growth factor stimulation. *J. Cell Biol.* 143:1535–1545.

Buss, F., S.D. Arden, M. Lindsay, J.P. Luzio, and J. Kendrick-Jones. 2001. Myosin VI isoform localized to clathrin-coated vesicles with a role in clathrin-mediated endocytosis. *EMBO J.* 20:3676–3684.

Chen, W.J., J.L. Goldstein, and M.S. Brown. 1990. NPXY, a sequence often found in cytoplasmic tails, is required for coated pit-mediated internalization of the low density lipoprotein receptor. *J. Biol. Chem.* 265:3116–3123.

Defacque, H., M. Egeberg, A. Habermann, M. Diakonova, C. Roy, P. Mangeat, W. Voelter, G. Marriott, J. Pfannstiel, H. Faulstich, and G. Griffiths. 2000. Involvement of ezrin/moesin in de novo actin assembly on phagosomal membranes. *EMBO J.* 19:199–212.

Folsch, H., H. Ohno, J.S. Bonifacino, and I. Mellman. 1999. A novel clathrin adaptor complex mediates basolateral targeting in polarized epithelial cells. *Cell*. 99:189–198.

Folsch, H., M. Pypaert, P. Schu, and I. Mellman. 2001. Distribution and function of AP-1 clathrin adaptor complexes in polarized epithelial cells. *J. Cell Biol.* 152:595–606.

Folsch, H., M. Pypaert, S. Maday, L. Pelletier, and I. Mellman. 2003. The AP-1A and AP-1B clathrin adaptor complexes define biochemically and functionally distinct membrane domains. *J. Cell Biol.* 163:351–362.

Gallione, C.J., and J.K. Rose. 1985. A single amino acid substitution in a hydrophobic domain causes temperature-sensitive cell-surface transport of a mutant viral glycoprotein. *J. Virol.* 54:374–382.

Gan, Y., T.E. McGraw, and E. Rodriguez-Boulan. 2002. The epithelial-specific adaptor AP1B mediates post-endocytic recycling to the basolateral membrane. *Nat. Cell Biol.* 4:605–609.

Grindstaff, K.K., C. Yeaman, N. Anandasabapathy, S.C. Hsu, E. Rodriguez-Boulan, R.H. Scheller, and W.J. Nelson. 1998. Sec6/8 complex is recruited to cell-cell contacts and specifies transport vesicle delivery to the basal-lateral membrane in epithelial cells. *Cell*. 93:731–740.

Guo, W., D. Roth, C. Walch-Solimena, and P. Novick. 1999. The exocyst is an effector for Sec4p, targeting secretory vesicles to sites of exocytosis. *EMBO J.* 18:1071–1080.

Hattula, K., and J. Peranen. 2000. FIP-2, a coiled-coil protein, links Huntingtin to Rab8 and modulates cellular morphogenesis. *Curr. Biol.* 10:1603–1606.

Hua, W., D. Sheff, D. Toomre, and I. Mellman. 2006. Vectorial insertion of apical and basolateral membrane proteins in polarized epithelial cells revealed by quantitative 3D live cell imaging. *J. Cell Biol.* 172:1035–1044.

Huber, L.A., S. Pimplikar, R.G. Parton, H. Virta, M. Zerial, and K. Simons. 1993. Rab8, a small GTPase involved in vesicular traffic between the TGN and the basolateral plasma membrane. *J. Cell Biol.* 123:35–45.

Hunziker, W., and C. Fumey. 1994. A di-leucine motif mediates endocytosis and basolateral sorting of macrophage IgG Fc receptors in MDCK cells. *EMBO J.* 13:2963–2969.

Ihrke, G., G.V. Martin, M.R. Shanks, M. Schrader, T.A. Schroer, and A.L. Hubbard. 1998. Apical plasma membrane proteins and endolyn-78 travel through a subapical compartment in polarized WIF-B hepatocytes. *J. Cell Biol.* 141:115–133.

Ihrke, G., S.R. Gray, and J.P. Luzio. 2000. Endolyn is a mucin-like type I membrane protein targeted to lysosomes by its cytoplasmic tail. *Biochem. J.* 345:287–296.

Ihrke, G., J.R. Bruns, J.P. Luzio, and O.A. Weisz. 2001. Competing sorting signals guide endolyn along a novel route to lysosomes in MDCK cells. *EMBO J.* 20:6256–6264.

Ihrke, G., A. Kyttala, M.R. Russell, B.A. Rous, and J.P. Luzio. 2004. Differential use of two AP-3-mediated pathways by lysosomal membrane proteins. *Traffic*. 5:946–962.

Kroschewski, R., A. Hall, and I. Mellman. 1999. Cdc42 controls secretory and endocytic transport to the basolateral plasma membrane of MDCK cells. *Nat. Cell Biol.* 1:8–13.

Lin, S., H.Y. Naim, A.C. Rodriguez, and M.G. Roth. 1998. Mutations in the middle of the transmembrane domain reverse the polarity of transport of the influenza virus hemagglutinin in MDCK epithelial cells. *J. Cell Biol.* 142:51–57.

Liu, J., D.W. Taylor, E.B. Krementsova, K.M. Trybus, and K.A. Taylor. 2006. Three-dimensional structure of the myosin V inhibited state by cryoelectron tomography. *Nature*. 442:208–211.

Marzolo, M.P., M.I. Yuseff, C. Retamal, M. Donoso, F. Ezquer, P. Farfan, Y. Li, and G. Bu. 2003. Differential distribution of low-density lipoprotein-receptor-related protein (LRP) and megalin in polarized epithelial cells is determined by their cytoplasmic domains. *Traffic*. 4:273–288.

Matter, K., W. Hunziker, and I. Mellman. 1992. Basolateral sorting of LDL receptor in MDCK cells: the cytoplasmic domain contains two tyrosine-dependent targeting determinants. *Cell*. 71:741–753.

Matter, K., E.M. Yamamoto, and I. Mellman. 1994. Structural requirements and sequence motifs for polarized sorting and endocytosis of LDL and Fc receptors in MDCK cells. *J. Cell Biol.* 126:991–1004.

Moritz, O.L., B.M. Tam, L.L. Hurd, J. Peranen, D. Deretic, and D.S. Papermaster. 2001. Mutant rab8 Impairs docking and fusion of rhodopsin-bearing post-Golgi membranes and causes cell death of transgenic *Xenopus* rods. *Mol. Biol. Cell*. 12:2341–2351.

Morris, S.M., S.D. Arden, R.C. Roberts, J. Kendrick-Jones, J.A. Cooper, J.P. Luzio, and F. Buss. 2002. Myosin VI binds to and localises with Dab2, potentially linking receptor-mediated endocytosis and the actin cytoskeleton. *Traffic*. 3:331–341.

Mostov, K.E., M. Verges, and Y. Altschuler. 2000. Membrane traffic in polarized epithelial cells. *Curr. Opin. Cell Biol.* 12:483–490.

Motley, A., N.A. Bright, M.N. Seaman, and M.S. Robinson. 2003. Clathrin-mediated endocytosis in AP-2-depleted cells. *J. Cell Biol.* 162:909–918.

Musch, A., D. Cohen, and E. Rodriguez-Boulan. 1997. Myosin II is involved in the production of constitutive transport vesicles from the TGN. *J. Cell Biol.* 138:291–306.

Musch, A., D. Cohen, G. Kreitzer, and E. Rodriguez-Boulan. 2001. cdc42 regulates the exit of apical and basolateral proteins from the trans-Golgi network. *EMBO J.* 20:2171–2179.

Muth, T.R., and M.J. Caplan. 2003. Transport protein trafficking in polarized cells. *Annu. Rev. Cell Dev. Biol.* 19:333–366.

Ohno, H., T. Tomemori, F. Nakatsu, Y. Okazaki, R.C. Aguilar, H. Foelsch, I. Mellman, T. Saito, T. Shirasawa, and J.S. Bonifacino. 1999. Mu1B, a novel adaptor medium chain expressed in polarized epithelial cells. *FEBS Lett.* 449:215–220.

Ostap, E.M. 2002. 2,3-Butanedione monoxime (BDM) as a myosin inhibitor. *J. Muscle Res. Cell Motil.* 23:305–308.

Paladino, S., T. Pocard, M.A. Catino, and C. Zurzolo. 2006. GPI-anchored proteins are directly targeted to the apical surface in fully polarized MDCK cells. *J. Cell Biol.* 172:1023–1034.

Pepperkok, R., J. Scheel, H. Horstmann, H.P. Hauri, G. Griffiths, and T.E. Kreis. 1993. Beta-COP is essential for biosynthetic membrane transport from the endoplasmic reticulum to the Golgi complex in vivo. *Cell*. 74:71–82.

Puri, C., D. Tosoni, R. Comai, A. Rabellino, D. Segat, F. Caneva, P. Luzzi, P.P. Di Fiore, and C. Tacchetti. 2005. Relationships between EGFR signaling-competent and endocytosis-competent membrane microdomains. *Mol. Biol. Cell*. 16:2704–2718.

Rodriguez-Boulan, E., G. Kreitzer, and A. Musch. 2005. Organization of vesicular trafficking in epithelia. *Nat. Rev. Mol. Cell Biol.* 6:233–247.

Roush, D.L., C.J. Gottardi, H.Y. Naim, M.G. Roth, and M.J. Caplan. 1998. Tyrosine-based membrane protein sorting signals are differentially interpreted by polarized Madin-Darby canine kidney and LLC-PK1 epithelial cells. *J. Biol. Chem.* 273:26862–26869.

Sahlender, D.A., R.C. Roberts, S.D. Arden, G. Spudich, M.J. Taylor, J.P. Luzio, J. Kendrick-Jones, and F. Buss. 2005. Optineurin links myosin VI to the Golgi complex and is involved in Golgi organization and exocytosis. *J. Cell Biol.* 169:285–295.

Sheff, D.R., R. Kroschewski, and I. Mellman. 2002. Actin dependence of polarized receptor recycling in Madin-Darby canine kidney cell endosomes. *Mol. Biol. Cell*. 13:262–275.

Shvartsman, D.E., M. Kotler, R.D. Tall, M.G. Roth, and Y.I. Henis. 2003. Differently anchored influenza hemagglutinin mutants display distinct interaction dynamics with mutual rafts. *J. Cell Biol.* 163:879–888.

Sugimoto, H., M. Sugahara, H. Folsch, Y. Koide, F. Nakatsu, N. Tanaka, T. Nishimura, M. Furukawa, C. Mullins, N. Nakamura, et al. 2002. Differential recognition of tyrosine-based basolateral signals by AP-1B subunit mu1B in polarized epithelial cells. *Mol. Biol. Cell*. 13:2374–2382.

Takeda, T., H. Yamazaki, and M.G. Farquhar. 2003. Identification of an apical sorting determinant in the cytoplasmic tail of megalin. *Am. J. Physiol. Cell Physiol.* 284:C1105–C1113.

Tall, R.D., M.A. Alonso, and M.G. Roth. 2003. Features of influenza HA required for apical sorting differ from those required for association with DRMs or MAL. *Traffic*. 4:838–849.

Thirumurugan, K., T. Sakamoto, J.A. Hammer III, J.R. Sellers, and P.J. Knight. 2006. The cargo-binding domain regulates structure and activity of myosin 5. *Nature*. 442:212–215.

Thomas, D.C., C.B. Brewer, and M.G. Roth. 1993. Vesicular stomatitis virus glycoprotein contains a dominant cytoplasmic basolateral sorting signal critically dependent upon a tyrosine. *J. Biol. Chem.* 268:3313–3320.

Wang, F., K. Thirumurugan, W.F. Stafford, J.A. Hammer III, P.J. Knight, and J.R. Sellers. 2004. Regulated conformation of myosin V. *J. Biol. Chem.* 279:2333–2336.

Warner, C.L., A. Stewart, J.P. Luzio, K.P. Steel, R.T. Libby, J. Kendrick-Jones, and F. Buss. 2003. Loss of myosin VI reduces secretion and the size of the Golgi in fibroblasts from Snell's waltzer mice. *EMBO J.* 22:569–579.

Wells, A.L., A.W. Lin, L.Q. Chen, D. Safer, S.M. Cain, T. Hasson, B.O. Carragher, R.A. Milligan, and H.L. Sweeney. 1999. Myosin VI is an actin-based motor that moves backwards. *Nature*. 401:505–508.

Zerial, M., and H. McBride. 2001. Rab proteins as membrane organizers. *Nat. Rev. Mol. Cell Biol.* 2:107–117.